Fe^{III} in high spin state in bis(5-bromosalicylaldehyde 4-ethylthiosemicarbazonato(1-)-κ^3-*O,N*^{1},*S*)ferrate(III) nitrate monohydrate, the first example of such a cationic Fe^{III} complex unit

Robyn E Powell[a,b], Martin R Lees[c], Graham J Tizzard[d] and Petra J van Koningsbruggen[a,b]*

[a] College of Engineering and Physical Sciences, School of Infrastructure and Sustainable Engineering Department of Chemical Engineering and Applied Chemistry, Aston University, Aston Triangle, Birmingham, West Midlands, B4 7ET, UK

[b]Aston Institute of Materials Research, Aston University, Birmingham B4 7ET, U.K

[c]Department of Physics, University of Warwick, Coventry CV4 7AL, UK

[d]National Crystallography Service, Chemistry, University of Southampton, Southampton, SO17 1BJ, UK

Correspondence email: p.vankoningsbruggen@aston.a.c.uk

Synopsis The $Fe^{III}S_2N_2O_2$ chromophore contains two O,N,S-donating monoanionic ligands in perpendicular planes with the O and S atoms in *cis* and the N atoms in *trans*-positions. The Fe^{III} ion is in the high spin state at 100 K.

Abstract The synthesis and crystal structure (100 K) of the title compound, $[Fe(H\text{-}5\text{-}Br\text{-}thsa\text{-}Et)_2](NO_3)\cdot H_2O$ (I), is reported. The asymmetric unit consists of an octahedral $[Fe^{III}(HL)_2]^+$ cation, where HL^- = H-5-Br-thsa-Et = 5-bromosalicylaldehyde 4-ethylthiosemicarbazonato(-1) (the correct IUPAC name for the ligand is 2-[(4-Ethylthiosemicarbazidoidene)methyl]-4- bromophenolate), a nitrate anion and a non-coordinated water molecule. Each L^- ligand binds with the thione-S, the imine-N and the phenolate-O as donor atoms resulting in an $Fe^{III}S_2N_2O_2$ chromophore. The O, N, S - ligands are orientated in two perpendicular planes with the O and S atoms in *cis* and the N atoms in *trans*-positions. This $[Fe(HL)_2](anion)\cdot H_2O$ compound contains the first known cationic Fe^{III} entity containing two salicylaldehyde thiosemicarbazone derivatives. The Fe^{III} ion is in the high spin state at 100 K. In addition, a comparative infrared spectroscopic study of the free ligand and the ferric complex is presented, demonstrating that such an analysis provides a quick identification of the degree of deprotonation and coordination mode of the ligand in this class of metal compounds. The variable-temperature magnetic susceptibility measurements (5-320 K) are consistent with the presence of a high spin Fe^{III} ion with a zero-field splitting D = 0.439(1) cm^{-1}.

1. Introduction

The history of Fe^{III} spin crossover compounds goes back to the 1930s when Cambi & Szegö observed temperature-dependent spin isomerism in iron(III) tris(dithiocarbamate) (Cambi & Szegö 1931; Cambi & Szegö 1933). Since then, two main families of Fe^{III} spin crossover systems have been extensively studied: those containing ligands sporting chalcogen donor atoms and those based on multidentate N,O-donating Schiff base-type ligands (van Koningsbruggen et al. 2004; Harding et al. 2016) and it has been found that the magnetic interconversion between the low spin (S = 1/2) and high spin (S = 5/2) state in Fe^{III} systems can be triggered by a change in temperature, pressure or by light irradiation (Hayami et al. 2000; van Koningsbruggen et al. 2004; Hayami et al. 2009; Harding et al. 2016).

Due to their switchable magneto-optical properties, various applications in the field of molecular electronics and sensing have been suggested for these bistable materials (Létard et al. 2004; Gütlich et al. 2004; Gütlich & Goodwin 2004; van Koningsbruggen et al. 2004; Takahashi et al., 2006; Halcrow 2013; Lefter et al., 2016; Molnar et al. 2018; Kumar et al. 2017; Rubio-Gimenez et al., 2019, Tissot et al., 2019, Karuppannan et al., 2021). Accordingly, in order to realise the full potential of spin crossover materials in applications, the quest for knowledge is focussed on how to use chemical synthesis in order to tune the spin transition characteristics such that the compounds can fulfil these particular functions.

Studies carried out by several research groups have demonstrated that R-salicylaldehyde 4R'-thiosemicarbazones are very versatile ligand systems that enable the tuning of the spin state of the Fe^{III} ion (van Koningsbruggen et al., 2004; W. Phonsri et al., 2017; Powell et al., 2014; Powell et al. 2015; Powell 2016; Powell et al. 2020; Powell et al. 2021; Yemeli Tido 2010; Zelentsov et al. 1973; Ryabova et al. 1978; Ryabova et al. 1981a; Ryabova et al. 1981b; Ryabova et al. 1982; Floquet et al. 2003; Floquet et al. 2006; Floquet et al. 2009; Li et al. 2013, Li et al. 2016). In spite of this versatility, in all instances the Fe^{III} isomer is identical in that the Fe^{III} ion is in a distorted $FeS_2N_2O_2$ octahedron formed by two tridentate O, N, S-ligands, which are geometrically arranged in such a way that the S and O atoms are located in *cis* positions, whereas the N atoms occupy *trans* positions, i.e. each tridentate ligand coordinates in an equatorial plane (van Koningsbruggen et al., 2004; W. Phonsri et al., 2017; Powell et al., 2014; Powell et al. 2015; Powell 2016; Powell et al. 2020; Powell et al. 2021; Yemeli Tido 2010; Zelentsov et al. 1973; Ryabova et al. 1978; Ryabova et al. 1981a; Ryabova et al. 1981b; Ryabova et al. 1982; Floquet et al. 2003; Floquet et al. 2006; Floquet et al. 2009; Li et al. 2013).

It has been demonstrated that the electronic state of an Fe^{III} ion surrounded by two of such tridentate O, N, S-thiosemicarbazonato ligands depends on the substituents and degree of deprotonation of the R-salicylaldehyde 4R'-thiosemicarbazone ligands, whereas the identity of the counter-ion, and the nature and degree of solvation afford further tuning of the Fe^{III} spin state (Powell *et al*. 2014; Powell *et al*. 2015; Powell, 2016; Powell *et al*. 2020; Powell *et al*. 2021; Yemeli Tido 2010). We made use of the

fact that in solution, the free R-salicylaldehyde 4R'-thiosemicarbazone ligand (H_2L) exists in two tautomeric forms *i.e*. the thione and thiol forms. Moreover, the ligand may also be present in its neutral, anionic or dianionic form. We established that the formation of a particular type of Fe^{III} complex unit, *i.e.* neutral, monocationic or monoanionic, can be achieved by tuning the degree of deprotonation of the ligand through pH variation of the reaction solution during the synthesis (Powell et al., 2014; Powell et al. 2015; Powell 2016; Powell et al. 2020; Powell et al. 2021; Yemeli Tido 2010; Floquet et al. 2009).

For this work, we used 5-bromosalicylaldehyde 4-ethylthiosemicarbazone (abbreviated as H_2-5-Br-thsa-Et), with the correct IUPAC name for the ligand being 2-[(4-Ethylthiosemicarbazidoidene)methyl]-4- bromophenol, whose two tautomeric forms, i.e. the thione and thiol forms, are shown in Scheme 1.

Our present research enlarges the scope for tuning the structure and spin state of Fe^{III} compounds of R-salicylaldehyde 4R'-thiosemicarbazones as we now report on $[Fe(H\text{-}5\text{-}Br\text{-}thsa\text{-}Et)_2](NO_3)\cdot H_2O$ (I) where H-5-Br-thsa-Et denotes 5-bromosalicylaldehyde 4-ethylthiosemicarbazonato(-1), which contains the first known cationic Fe^{III} complex entity containing two salicylaldehyde thiosemicarbazone derivatives. Its structure was determined at 100 K and confirmed that Fe^{III} is in the high spin state. Furthermore, an infrared spectroscopic characterisation of the free ligand and the ferric complex is presented together with a variable-temperature magnetic susceptibility study.

2. Experimental Details

2.1 Spectroscopic and Magnetic Measurements

A room temperature IR spectrum of 5-bromosalicylaldehyde 4-ethylthiosemicarbazone within the range 4000-400 cm^{-1} was recorded on a Perkin Elmer FT-IR spectrometer Spectrum RXI by using KBr pellets. IR spectroscopic measurements of $[Fe(H\text{-}5\text{-}Br\text{-}thsa\text{-}Et)_2](NO_3)\cdot H_2O$ within the range 4000-600 cm^{-1} were carried out at room temperature using an ATR (Attenuated Total Reflectance) Perkin Elmer FT-IR Frontier spectrometer.

^1H and ^{13}C NMR spectra were recorded in DMSO-d_6 using a BRUKER cryomagnet BZH 300/52 spectrometer (300 MHz) with the recorded chemical shifts in δ (in parts per million) relative to an internal standard of TMS (tetramethylsilane).

Measurements of dc magnetic susceptibility, χ_M, versus temperature, T, were conducted between 5 - 320 K heating at a rate of 2 K min^{-1} in an applied field, $\mu_0 H$, of 0.1 T using a Quantum Design MPMS-5S SQUID (Superconducting Quantum Interference Device) magnetometer. The SQUID

magnetometer was calibrated using a standard palladium sample. The background due to the sample holder and the diamagnetic signal of the sample, estimated using Pascal's constants (Bain et al. 2008), were subtracted from the measured molar magnetic susceptibility χ_M.

2.2 Synthesis

The synthesis of 5-bromosalicylaldehyde 4-ethylthiosemicarbazone (H_2-5-Br-thsa-Et) has been carried out as follows: 49 mmol (9.85 g) of 5-bromo-salicylaldehyde was dissolved in 80 mL of ethanol with constant stirring, and was added to 49 mmol (5.84 g) of 4-ethyl-3-thiosemicarbazide dissolved in 40 mL of ethanol. The corresponding mixture was refluxed for 120 minutes. The resulting solution was cooled to room temperature, the solid isolated by filtration, washed with ether and dried in a vacuum for two days. Yield: 14.32 g (47.55 mmol, 97.0%). Mp: 186°C. H_2-5-Br-thsa-Et is soluble in methanol, acetone and DMSO. ^{1}H NMR (300 MHz, DMSO-d_6) δ (ppm): 11.42 (1H, s, OH), 10.28 (1H, s, S=C−NH), 8.32 (1H, m, N=CH), 8.66 (1H, t, S=C−NH(CH_2CH_3)), 6.80-7.38 (aromatic 3H, m, C−H), 3.60 (2H, p, NH−CH_2), 1.15 (3H t, NHCH_2−CH_3). ^{13}C NMR (300 MHz, DMSO-d_6) δ (ppm): 176.5 (C=S), 155.5 (C−O), 137.0 (C=N), 133.2, 128.1, 122.9, 118.2 (C−C aromatic), 110.9 (C−Br), 38.2 (CH_2), 14.8 (CH_3). IR (cm^{-1}, KBr): 3299 (νOH), 3146 (νNH), 2990 (νCH_3), 2936 (νCH_2), 1613 (νC=N), 1601, 1550 (νC=C), 1237 (νC−N), 1047 (νC=S).

The synthesis of [Fe(H-5-Br-thsa-Et)$_2$](NO_3)·H_2O has been carried out as follows: Fe(NO_3)$_3$·9H_2O (1.0 mmol, 0.40 g) was dissolved in 5 mL of distilled water. The ligand H_2-5-Br-thsa-Et (2.0 mmol, 0.60 g) was dissolved in an ethanol/methanol/water mixture (v: v: v, 5: 5: 1) with the addition of dimethylamine, 40wt% in water (10 mmol, 0.51 mL). To this mixture, the Fe(III) salt solution was added dropwise on constant stirring. The resulting dark green solution was stirred and heated to 120 °C for approximately 10 minutes. The solution was then allowed to stand at room temperature until crystals were formed. The dark green microcrystals were isolated by filtration and dried. Yield: 0.54 g (0.73 mmol, 73.2%). IR (cm^{-1}, ATR): 3313, 3225.8 (νNH), 3047 (νCH_3), 2997 (νCH_2), 1601 (νC=N), 1582, 1542 (νC=C ring), 1294 (νC−O), 1312 (νN−N), 819 (νC−S), 867, 1352 (νNO).

2.3 Refinement

Crystal data, data collection and structure refinement details are summarised in Table 1. The hydrogen atoms H10B and H10A of the water solvent molecule were located at idealised geometrical positions and refined with the riding model with U_{iso}(H) = 1.5U_{eq}(O). The water molecule was then refined as a rigid group using the AFIX 6 command. The hydrogen atoms bonded to nitrogen atoms, H12, H13, H21 and H22 were located in the difference map and refined riding on their parent atoms with U_{iso}(H) = 1.2U_{eq}(N). All other hydrogen atoms were included in the refinement in calculated positions, and

riding on their parent atoms, C–H = 0.95 Å and U_{iso}(H) = 1.2U_{eq}(C), C–H = 0.99 Å and U_{iso}(H) = 1.2U_{eq}(C), C–H = 0.98 Å and U_{iso}(H) = 1.5U_{eq}(C) for the methine (-CH=), methylene (-CH_2-) and methyl (-CH_3) hydrogen atoms, respectively. Additional details towards the structure refinement of [Fe(H-5-Br-thsa-Et)$_2$](NO_3)·H_2O are as follows: the *SMTBX* solvent masking routine as implemented within Olex2 was used to mask residual electron density from unidentified solvent (Dolomanov et al., 2009). A solvent mask was calculated, and 116 electrons were found in four voids per unit cell with a combined volume of 360 Å^3. This is consistent with the presence of 0.375[EtOH], 0.125[MeOH] and 0.25[H_2O] per asymmetric unit which accounts for 116 electrons per unit cell. These proportions are an estimate and not all of the solvents are necessarily present, so this estimate has not been included in the structural or moiety formulae. The program used for the structure solution: *SHELXT* 2018/2 (Sheldrick, 2015); the structure refinement used the program *SHELXL* 2018/3 (Sheldrick, 2015). The *OLEX2* (Dolomanov et al., 2009). and *ORTEP-3* for Windows (Farrugia, 2012) programs were used to produce the molecular graphics.

3 Results and discussion

In solution the free ligand, 5-bromosalicylaldehyde 4-ethylthiosemicarbazone (H_2L), exists in two tautomeric forms, i.e. the thione and the thiol form as illustrated in Scheme 1. Consequently, in Fe^{III} compounds the ligand may be present in either one of the possible tautomers, and may be neutral, anionic, or dianionic. Referring to the thiol tautomer, the neutral 5-bromosalicylaldehyde 4-ethylthiosemicarbazone (H_2L) has hydrogen atoms located on the phenol-oxygen and the thiol-sulphur. The first deprotonation step involving the phenol group results in the formation of 5-bromosalicylaldehyde 4-ethylthiosemicarbazone(-1) (abbreviated as $HL^{—}$). Subsequent deprotonation yields 5-bromosalicylaldehyde 4-ethylthiosemicarbazonato(-2) (abbreviated as $L^{2—}$).

The crystal structure of bis(5-bromosalicylaldehyde 4-ethylthiosemicarbazonato(1-)-κ^3-*O,N^1,S*)ferrate(III) nitrate monohydrate, [Fe(H-5-Br-thsa-Et)$_2$](NO_3)·H_2O (Figure 1), was determined at 100 K. The present compound crystallises in the orthorhombic system in the space group *Pnna*. The asymmetric unit is comprised from the [Fe(H-5-Br-thsa-Et)$_2$]$^+$ cation, a nitrate anion and a water solvent molecule and further ethanol, methanol and water in unknown proportions. To our knowledge, this is the first structure that is reported of a cationic Fe^{III} complex entity containing two salicylaldehyde thiosemicarbazone derivatives. Selected geometric parameters are given in Table 2. The Fe^{III} cation is coordinated by two singly deprotonated thione O,N,S-ligands. The 5-bromosalicylaldehyde 4-ethylthiosemicarbazonato(1-) ligands are deprotonated at the phenolate-O atoms.

The $Fe^{III}O_2N_2S_2$ unit displays a distorted octahedral geometry, as corroborated by the bond angles involving the ligand donor atoms and the Fe1 atom.

The Fe1 donor atom distances involving the two tridentate anionic H-5-Br-thsa-Et ligands are Fe1–S11 = 2.4404(15) Å, Fe1–S21 = 2.4615(14) Å, Fe1–O11 = 1.952(3) Å, Fe1–O21 = 1.944(3) Å, Fe1–N11 = 2.176(4) Å and Fe1–N21 = 2.161(4) Å for the bond distances from Fe^{III} to thione-S, phenolate-O and imine-N atoms of the two crystallographically independent ligands. The Fe-donor atom bond distances suggest that the Fe^{III} cation in the present compound is in the high spin state at 100 K. In fact, these bond distances compare rather well to these involving high spin Fe^{III} in $(CH_3)_2NH_2[Fe(3\text{-OEt-thsa})_2]$ (3-OEt-thsa = 3-ethoxy-salicylaldehyde thiosemicarbazonato(-2)) determined at 100 K, i.e. Fe1–S1 = 2.4320(6) Å, Fe1–S101 = 2.4389(7) Å, Fe1–O1 = 1.9806(16) Å, Fe1–O101 = 1.9595(16) Å, Fe1–N1 = 2.167(2) Å and Fe1–N101 = 2.131(2) Å for the bond distances from Fe^{III} to thiol-S, phenolate-O and imine-N atoms of the two crystallographically independent ligands (Powell et al., 2021). In fact, typical distances for Fe–S, Fe–O and Fe–N bonds are 2.23-2.31, 1.93-1.95 and 1.88-1.96 Å, respectively, for low spin Fe^{III} in compounds of formula (cation^{+})[Fe(R-salicylaldehyde 4R'-thiosemicarbazonato^{2-})$_2$]·x(solvent), and 2.40-2.44, 1.96-1.99 and 2.05-2.15 Å, respectively, for the corresponding high spin Fe^{III} compounds (van Koningsbruggen et al., 2004), albeit that the Fe^{III}-S distance involves the thiol moiety rather than the thione entity that is present in the title compound. Variable temperature magnetic susceptibility measurements (5-300 K) confirm that the Fe^{III} ion in this compound is indeed in the high spin state over this temperature range (*vide infra*) (Powell, 2016).

The tridentate ligands in the present compound coordinate to the Fe^{III} cation to give rise to an $Fe^{III}O_2N_2S_2$ octahedral environment, forming six- and five-membered chelate rings. The values of the root-mean-square deviations from the least-squares planes of the atoms comprising the five membered [Fe1 N11 N12 C18 S11] and [Fe1 N21 N22 C28 S21] chelate rings are 0.071 Å and 0.007 Å, respectively; the corresponding values for the six-membered [Fe1 N11 C17 C11 C12 O11] and [Fe1 N21 C27 C21 C22 O21] chelate rings are 0.073 Å and 0.102 Å, respectively. These geometric features are associated with O11–Fe1–N11 and O21–Fe1–N21 bite angles of 83.71(14)° and 83.82(14)°, respectively; as expected the six-membered chelate ring's bite angles are larger than the values of the five-membered chelate ring's bite angles of S11–Fe1–N11 = 79.00(11)° and S21–Fe1–N21 = 79.05(11)°. The conformation of the five- and six-membered chelate rings of [Fe(H-5-Br-thsa-Et)$_2$](NO_3)·H_2O is such that there is no major puckering.

5-Bromosalicylaldehyde 4-ethylthiosemicarbazone appears to be in its thione form, *i.e.* it is deprotonated at the phenolate-O atoms (O11 and O21) and possesses a hydrogen atom on the hydrazinic nitrogen atoms (N12 and N22). The protonation of the hydrazinic N atoms (N12 and N22) confirms the presence of the thione form of the tautomer, which is corroborated by the C=S bond distances of the 5-bromosalicylaldehyde 4-ethylthiosemicarbazonato(1-) ligands being closer to those having a C=S bond order of two. The C–S bond distances are C18–S11 = 1.692(5) Å and C28–S21 = 1.698(5) Å. Furthermore, electron delocalisation over the 5-membered chelate involving each ligand is inferred from the values for the N–N and C–N bond distances of each ligand that is coordinated to the Fe^{III}

cation. These bond distances are indicative of a bond order higher than one, *i.e*. the N11–N12 and N21–N22 bond distances are 1.396(6) Å and 1.376(6) Å, respectively, and the N12–C18 and N22–C28 bond distances are 1.349(6) Å and 1.352(6) Å, respectively.

The hydrogen bonding interactions of $[Fe(H\text{-}5\text{-}Br\text{-}thsa\text{-}Et)_2](NO_3)\cdot H_2O$ are listed in Table 3 and displayed in Figure 2. The nitrate anion is involved in hydrogen bonding interactions with the 5-bromosalicylaldehyde 4-ethylthiosemicarbazonato(1-) ligand. These hydrogen bonding interactions include the ligands' terminal nitrogen atoms N13 and N23 forming contacts with the oxygen atoms of the nitrate anion, O203 and $O201^{i}$ (i = -1 + x, 3/2 – y, 3/2 – z), respectively. The ligand's nitrogen atom N12 forms a contact N12–H12···O202 with the oxygen atom O202 of the nitrate anion. Also, the nitrate anion forms a hydrogen bonding interaction with the oxygen atom $O101^{i}$ (i = -1/2 + x, + y, 1 – z) of the water solvent molecule. Therefore, the nitrate anion is involved in two hydrogen bonding ring systems which connect the Fe^{III} units. The first ring system is formed between two Fe^{III} units, two water solvent molecules and a nitrate anion. The ring system is formed by the following contacts N12–H12···O202, O101–H10A···$O202^{i}$ (i = -1/2 + x, + y, 1 – z), O101–H10B···O11and N22–H22···$O101^{i}$ (i = -1/2 + x, + y, 1 – z), giving rise to a $R^5_4(18)$ ring system. Furthermore, the second ring system is created by the contacts N12–H12···O202 and N13–H13···O203, giving rise to a $R^2_2(8)$ ring system. The structure does include a halogen…chalcogen contact ($Br21\cdots S11^{i}$ = 3.5103(13) Å, (i = 1 – x, 1 – y, 1 – z)) and halogen…halogen contact ($Br11\cdots Br11^{i}$ = 3.5999(11) Å, (i = 5/2 – x, 2 – y, + z)) less than the sum of the VdW radii.

The assembly of the Fe^{III} units of the present compound is displayed in Figure 3. The presence of both the NO_3^- anion and the water solvent molecule of $[Fe(H\text{-}5\text{-}Br\text{-}thsa\text{-}Et)_2](NO_3)\cdot H_2O$ co-determines how the Fe^{III} units are packed in the crystal lattice. $[Fe(H\text{-}5\text{-}Br\text{-}thsa\text{-}Et)_2](NO_3)\cdot H_2O$ displays $Fe^{III}\cdots Fe^{III}$ (1/2 + x, y, –z + 1) separations of 6.7661(7) Å and $Fe^{III}\cdots Fe^{III}$ (x, 1/2 – y, 3/2 – z) separations of 7.2104(16) Å. Despite the presence of the water solvent molecule and the nitrate anion the Fe^{III} units are packed relatively close together within the crystal lattice. This feature could be due to the hydrogen bonding ring systems (*vide supra*), which link the Fe^{III} units together using the hydrogen bonding interactions of the water solvent molecule and the nitrate anion.

An infrared spectroscopic characterisation of the free ligand has been carried out, as well as a comparison with the IR spectrum of the ferric complex in order to assess the degree of deprotonation and the coordination mode of the ligand.

The infrared spectrum of the free ligand, 5-bromosalicylaldehyde 4-ethylthiosemicarbazone (H_2-5-Br-thsa-Et), exhibits a strong band at 1613 cm^{-1}, which is assigned to the imine group that has been formed during the ligand synthesis, which involves the condensation of the salicylaldehyde moiety and the thiosemicarbazone moiety. Furthermore, the infrared spectrum of the ligand exhibits a medium band at 3146 cm^{-1}, which is assigned to the νN–H vibration. The presence of the νN–H band in the spectrum of $[Fe(H\text{-}5\text{-}Br\text{-}thsa\text{-}Et)_2](NO_3)\cdot H_2O$ evidences that the thione form of the ligand is coordinated to the

central Fe^{III} cation. Upon coordination of the imine nitrogen, the νC=N band shifts from 1613 cm^{-1} in the free ligand to 1600 cm^{-1} in the complex. The νN–N band of the thiosemicarbazone moiety of the free ligand is found at 1105 cm^{-1}; the wavenumber increases to 1312 cm^{-1} for the νN–N band in the ferric complex. In comparison to the free ligand, the ferric complex does not show the presence of the νOH vibration; this is due to the phenolic oxygen having been deprotonated in order to coordinate the O,N,S-tridentate chelating ligand to the Fe^{III} cation in the $[Fe(H\text{-}5\text{-}Br\text{-}thsa\text{-}Et)_2]^+$ cation. The corresponding νOH band for the free ligand is found at 3299 cm^{-1}. The Fe^{III} cation is also coordinated to the sulphur atom of the thiosemicarbazone moiety of the ligand. The νCS band of the ligand that is coordinated to the Fe^{III} ion is assigned at 819 cm^{-1} in the ferric complex, but it is at a larger wavenumber in the free ligand, *i.e.* νCS at 1046 cm^{-1}. The decrease in the frequency of the νCS band in the thiosemicarbazone upon complexation of the ligand indicates coordination of the thione-S atom to the Fe^{III} cation. The results of our analysis will be instrumental for the quick identification of the degree of deprotonation and coordination mode of the ligand in future metal compounds as it is based on easily accessible IR spectroscopic measurements.

In the infrared spectrum of the ferric complex there are two bands which represent the presence of the nitrate anion within the crystal lattice, the νNO bands of the NO_3^- anion are assigned at 866 and 1352 cm^{-1}, respectively. Furthermore, as evidenced from the crystallographic study of the complex $[Fe(H\text{-}5\text{-}Br\text{-}thsa\text{-}Et)_2](NO_3)\cdot H_2O$ there is hydrogen bonding within the crystal lattice; this is supported by the broad peaks observed for the νNH bands assigned to the azomethine and terminal nitrogen atoms of the thiosemicarbazone moiety of the coordinated ligand.

Variable temperature magnetic susceptibility measurements (5 - 320 K) were carried out in order to confirm the spin state of the Fe^{III} ion. The temperature dependence of $\chi_M T$ for $[Fe(H\text{-}5\text{-}Br\text{-}thsa\text{-}Et)_2](NO_3)\cdot H_2O$ is displayed in Figure 4(a). $\chi_M T$ varies from 3.27 $cm^3\ mol^{-1}$ K at 5 K to an almost constant value of 4.33(1) $cm^3\ mol^{-1}$ K [5.89(1)μ_B/Fe] at higher temperatures (50 - 320 K). This is close to the expected value of 4.37 $cm^3\ mol^{-1}$ K [5.92μ_B/Fe] for Fe^{III} in its high spin state (S = 5/2) with an electronic g-factor of 2.0023. A Curie-Weiss behaviour at high temperature is confirmed by the linear behaviour of $\chi_M^{-1}(T)$, and the fit to a Curie-Weiss law shown in Figure 4(b) between 100 and 320 K gives a Weiss temperature of -0.5(1) K and an effective moment of 5.86(1)μ_B/Fe.

$\chi_M T$ drops rapidly below 20 K reflecting a significant zero-field splitting of the S = 5/2 state. The spin Hamiltonian can be written as $H_S = H_{CEF} + H_z$. The crystalline electric field term $H_{CEF} = D[S_z^2\text{-}S(S+1)/3] + E(S_x^2 - S_y^2)$, where D and E are the axial and rhombic zero-field splitting, respectively. The ^6S high spin state is split into 3 Kramers doublets with the higher levels separated by 2D and 6D from the lowest energy level. The Zeeman energy $H_z = g\mu_B H S_x$ and then the molar magnetic susceptibility for E = 0 is

$$\chi_M = \frac{N_A g^2 \mu_B^2}{4k_B T}\left[\frac{1 + 9e^{-2X} + 25e^{-6X}}{1 + e^{-2X} + e^{-6X}}\right], \quad \text{Eqn (1)}$$

where $X = D/k_BT$, N_A is Avogadro's number and k_B is the Boltzmann constant. A least-squares fit gives $D = 0.439(1)$ cm^{-1} with $g = 2$. This is in the range expected for high spin Fe^{III} (Chen *et al*., 2002, Yemeli Tido *et al*., 2007). Fits with a finite E expected for a system with a rhombic distortion are possible, cf. Chen *et al*., 2002, but these require a knowledge of the ratio $\lambda = E/D$ from other studies, e.g. electron paramagnetic resonance spectroscopy or inelastic neutron scattering, and lower temperature magnetic susceptibility data.

We thus reported the first structural characterisation of a member of the family of $[Fe(HL^{-})_2](anion^{-})\cdot n(solvent)$ (H_2L = R-salicylaldehyde 4R'-thiosemicarbazone) compounds, which contains a cationic Fe^{III} entity. This further demonstrated the large versatility in charge distribution that can be achieved using this ligand system as neutral Fe^{III} complex units have been previously observed for $[Fe(HL^{-})(L^{2-})]\cdot n(solvent)$, whereas anionic Fe^{III} units have been found to be present in $(cation^{+})[Fe(L^{-})_2]\cdot n(solvent)$ (van Koningsbruggen et al., 2004; W. Phonsri et al., 2017; Powell et al., 2014; Powell et al. 2015; Powell 2016; Powell et al. 2020; Powell et al. 2021; Yemeli Tido 2010; Zelentsov et al. 1973; Ryabova et al. 1978; Ryabova et al. 1981a; Ryabova et al. 1981b; Ryabova et al. 1982; Floquet et al. 2003; Floquet et al. 2006; Floquet et al. 2009; Li et al. 2013).

The Fe^{III} ion is the high spin state throughout the temperature range (5 - 320 K) over which the magnetic susceptibility data have been recorded. Since this compound is the first exponent of a cationic Fe^{III} entity of this family, it is too early to attempt to relate the structural and electronic features of the material to the nature of the Fe^{III} spin state and to comment on the reasons for the absence of Fe^{III} spin-crossover. This as yet limited knowledge related to the present material is not unexpected as also for the relatively well-known family of $(cation^{+})[Fe(L^{2-})_2]$ compounds of which several members have been structurally and magnetically characterised (van Koningsbruggen et al., 2004; W. Phonsri et al., 2017; Powell et al., 2014; Powell et al. 2015; Powell 2016; Powell et al. 2020; Powell et al. 2021; Yemeli Tido 2010; Zelentsov et al. 1973; Ryabova et al. 1978; Ryabova et al. 1981a; Ryabova et al. 1981b; Ryabova et al. 1982; Floquet et al. 2003; Floquet et al. 2006; Floquet et al. 2009; Li et al. 2013, Li et al. 2016), a correlation between structure and Fe^{III} spin state, including the occurrence of spin-crossover behaviour, could as yet not be established. The reasons for this incomplete understanding lie in the occurrence of a spin transition being governed by subtle structural and electronic modifications that are also tuned by the crystal packing, which in concert determine the ligand field strength and hence the manifestation of spin-crossover behaviour. These modifications depend on the nature of the ligands, the non-coordinating cation, the solvent molecules (if any), and the crystal packing. Clearly, the stabilisation of Fe^{III} in a particular spin state is governed by a subtle balance of electronic and geometric parameters, as is implied by the fact that a single compound ($NH_4[Fe(5\text{-Br-thsa})_2]$ (Ryabova et al., 1981b)) exists in slightly different polymorphs each with its distinct magnetic behaviour.

Our further research will focus on investigating the modulation of the Fe^{III} spin state upon varying the R,R'-substituents of the ligand, the non-coordinating anion, the degree of solvation and intermolecular

interactions in such $[Fe(HL^{-})_2](anion^{-})\cdot n(solvent)$ (H_2L = R-salicylaldehyde 4R'-thiosemicarbazone) compounds with the objective of defining the parameters for generating spin crossover behaviour in these systems.

Acknowledgements We thank the EPSRC UK National Crystallography Service (Coles & Gale, 2012) at the University of Southampton for the collection of the crystallographic data.

References

Bain, G.A, and Berry, J. F. (2008) *J. Chem. Educ.* **85** 532-536.

Cambi, L. & Szegö, L. (1931). *Ber.*, **64**, 2591-2598.

Cambi, L. & Szegö, L. (1933). *Ber.*, **66**, 656-661.

Chen, C.-H., Lee, Y.-Y., Liau, B.-C., Shanmugham, E., Chen, J.-H., Hsieh, H.-Y, Liao, F.-L. Wang, S.-L. & Hwang, L.-P. (2002). *J. Chem. Soc., Dalton. Trans*., 3001-3006.

Coles, S. J. & Gale, P. A. (2012). *Chem. Sci.,* **3**, 683-689.

CrysAlisPro, (2014). Agilent Technologies, Version 1.171.37.31, 2014.

Dolomanov, O. V., Bourhis, L. J., Gildea, R. J., Howard, J. A. K. & Puschmann, H. (2009). J. Appl. Cryst. **42**, 339-341.

Farrugia, L. J. (2012). J. Appl. Cryst. **45**, 849-854.

Floquet, S., Boillot, M. L., Rivière, E., Varret, F., Boukheddaden, K., Morineau, D. & Négrier, P. (2003). *New J. Chem.*, **27**, 341-348.

Floquet, S., Guillou, N., Négrier, P., Rivière, E., & Boillot, M. L. (2006). *New J. Chem.*, **30**, 1621-1627.

Floquet, S., Muñoz, M. C., Guillot, R., Rivière, E., Blain, G., Real, J. A., & Boillot, M. L. (2009). *Inorg. Chim. Acta*, **362**, 56-64.

Gütlich, P. & Goodwin, H. A. (2004). *Top. Curr. Chem.*, **233**, 1-47.

Gütlich, P., Koningsbruggen, P. J. van & Renz, F. (2004). *Struct. Bond.*, **107**, 27-75.

Halcrow, M.A. (Ed.) (2013). *Spin-Crossover Materials*; John Wiley & Sons, Ltd.: Oxford, UK.

Harding, D. J., Harding, P. & Phonsrib, W., (2016). *Coord. Chem. Rev*., **313**, 38-61.

Hayami, S., Gu, Z., Shiro, M., Einaga, Y., Fujishima, A., & Sato, O. (2000). *J. Am. Chem. Soc.*, **122**, 7126-7127.

Hayami, S., Hiki, K., Kawahara, T., Maeda, Y., Urakami, D., Inoue, K., Ohama, M., Kawata, S., & Sato, O. (2009). *Chem. Eur. J.*, **15**, 3497-3508.

Karuppannan, S. K, Martín-Rodríguez, A., Ruiz, E., Harding, P., Harding, D. J., Yu, X., Tadich, A., Cowie, B., Qi, D. & Nijhuis, C. A., (2021). *Chem. Sci*., **12**, 2381-2388.

Koningsbruggen, P. J. van, Maeda, Y. & Oshio, H. (2004). *Top. Curr. Chem.*, **233**, 259-324.

Kumar, K. S. & Ruben M. (2017). *Coord. Chem. Rev.,* **346**, 176-205.

Lefter, C., Vincent Davesne, V., Salmon, L., Molnár, G., Demont, P., Rotaru, A. & Bousseksou, A. (2016). *Magnetochemistry*. **2**, 18.

Létard, J. F., Guionneau, P. & Goux-Capes, L. (2004). *Top. Curr. Chem.*, **235**, 221-249.

Li Z. Y., Dai, J. W., Shiota, Y., Yoshizawa, K., Kanegawa, S. & Sato, O. (2013). *Chem. Eur. J.*, **19**, 12948-12952.

Li, Z.-Y., Ohtsu, H., Kojima, T., Dai, J.-W., Yoshida, T., Breedlove, B. K., Zhang, W.-X., Iguchi, H., Sato, O., Kawano, M. & Yamashita, M. (2016). *Angew. Chem. Int. Ed*., **55**, 5184-5189.

Molnar, G., Rat, S., Salmon, L., Nicolazzi, W. & Bousseksou, A. (2018). *Adv. Mater*., **30**, 1703862.

Palatinus, L. & Chapuis, G. (2007). *J. Appl. Cryst*., **40**, 786-790.

Phonsri, W., Darveniza, L. C., Batten, S. R. & K. S. Murray (2017). *Inorganics*, **5**, 51.

Powell, R. E., Schwalbe, C. H., Tizzard, G. J. & van Koningsbruggen, P. J. (2014). *Acta Crystallogr. C*., **C70**, 595–598.

Powell, R. E., Schwalbe, C. H., Tizzard, G. J. & van Koningsbruggen, P. J. (2015). *Acta Crystallogr. C*., **C71**, 169-174.

Powell, R.E. (2016). *Structures and Magnetic Properties of Iron(III) Spin-Crossover Compounds*, PhD Thesis, Aston University, Birmingham, United Kingdom.

Powell, R. E., Stöger, B., Knoll, C. Müller, D., Weinberger, P. & van Koningsbruggen, P. J. (2020). *Acta Crystallogr. C*., **C76**, 625–631.

Powell, R. E., C. H., Tizzard, G. J. & van Koningsbruggen, P. J. (2021). *Acta Crystallogr. C*., To be submitted for Publication.

Riguku Corporation. (2013). *CrystalClear-SM Expert 2.1 b29*, The Woodlands, Texas, U.S.A.

Rigaku Oxford Diffraction. (2021). *CrysAlisPro 1.171.41.120a*, Wroclow, Poland

Rubio-Gimenez, V., Bartual-Murgui, C., Galbiati, M., Núñez-López, A., Castells-Gil, J., Quinard, B., Seneor, P., Otero, E., Ohresser, P., Cantarero, A., Coronado, E., Real, J. A., Mattana, R., Tatay, S. & Martí-Gastaldo, C. (2019). *Chem. Sci*., **10**, 4038-4047.

Ryabova, N. A., Ponomarev, V. I., Atovmyan, L. O., Zelentsov, V. V. & Shipilov, V. I. (1978). *Koord. Khim.*, **4**, 119.

Ryabova, N. A., Ponomarev, V. I., Zelentsov, V. V. & Atovmyan, L. O. (1981a). *Kristallografiya*, **26**, 101-108.

Ryabova, N. A., Ponomarev, V. I., Zelentsov, V. V., Shipilov, V. I. & Atovmyan, L. O. (1981b). *J. Struct. Chem.*, **22**, 234-238.

Ryabova, N. A., Ponomarev, V. I., Zelentsov, V. V. & Atovmyan, L. O. (1982). *Kristallografiya*, **27**, 81-91.

Sheldrick, G.M. (2015). *Acta Cryst.* **A71**, 3-8.

Takahashi, K., Cui, H.-B., Okano, Y., Kobayashi, H., Einaga, Y., Sato, O. (2006). *Inorg., Chem*., **45**, 5739-5741.

Tissot, A., Kesse, X., Giannopoulou, S., Stenger, I., Binet, L., Rivière, E. & Serre, C. (2019). Chem. Commun., 55, 194-197.

Yemeli Tido, E.W., Vertelman, E. J. M., Meetsma, A. & van Koningsbruggen, P. J. (2007). *Inorg. Chim. Acta*, **360**, 3896-3902.

Yemeli Tido, E. W. (2010). *Synthesis and Characterisation of Molecular Magnetic Switches*, PhD Thesis, University of Groningen, The Netherlands.

Zelentsov, V. V., Bogdanova, L. G., Ablov, A. V., Gerbeleu, N. V. & Dyatlova, C. V. (1973). *Russ. J. Inorg. Chem.*, **18**, 2654-2657.

Table 1 Experimental Details

Crystal data	
Chemical formula	$[Fe(H\text{-}5\text{-}Br\text{-}thsa\text{-}Et)_2](NO_3)\cdot H_2O$ [+ solvent]
M_r	738.25
Crystal system, space group	Orthorhombic, *Pnna*
Temperature (K)	100(2)
a, *b*, *c* (Å)	12.3595(3), 23.2686(6), 19.6406(6)
α, β, γ (°)	90, 90, 90
V (Å^3)	5648.4(3)
Z	8
Radiation type	Mo *K*α
μ (mm^{-1})	3.559
Crystal size (mm)	0.19 x 0.01 x 0.01
Data collection	
Diffractometer	Rigaku AFC12 four-circle Kappa diffractometer
Absorption correction	Multi-scan CrysAlisPro (Rigaku OD, v.1.171.41.12a, 2021)
T_{min}, T_{max}	0.73967, 1.000
No. of measured, independent and observed [$I > 2\sigma(I)$] reflections	36848, 6477, 4297
R_{int}	0.0875
$(\sin\theta/\lambda)_{max}$ (Å^{-1})	0.649
Refinement	
$R[F^2 > 2\sigma(F^2)]$, $wR(F^2)$, S	0.0572, 0.1300, 1.014

No. of reflections	6477
No. of parameters	360
No. of restraints	6
H-atom treatment	H atoms treated by a mixture of independent and constrained refinement
$\Delta\rho_{max}$, $\Delta\rho_{min}$ (e Å^{-3})	0.683, -0.779

Diffractometer: *Rigaku AFC12* goniometer equipped with an enhanced sensitivity (HG) *Saturn724+* detector mounted at the window of an *FR-E+ SuperBright* molybdenum rotating anode generator with HF *Varimax* optics. **Cell determination and data collection**: *CrystalClear-SM Expert 3.1 b27* (Rigaku, 2013). **Data reduction, cell refinement and absorption correction**: *CrysAlisPro 1.171.141.120a* (Rigaku OD, 2021). **Structure solution**: *SHELXT 2018/2* (Sheldrick (2015). **Structure refinement**: *SHELXL 2018/3* (Sheldrick (2015)). **Graphics:** *OLEX2* (Dolomanov *et al.* (2009)), *ORTEP-3* for Windows (Farrugia, (2012)).

Table 2

Selected geometric parameters (Å, °)

Fe1–S11	2.4404(15)	Fe1–S21	2.4615(14)
Fe1–O11	1.952(3)	Fe1–O21	1.944(3)
Fe1–N11	2.176(4)	Fe1–N21	2.161(4)
S11–Fe1–S21	98.70(5)	O11–C12–C11	123.0(5)
S11–Fe1–N11	79.00(11)	C12–C11–C17	124.1(5)
S11–Fe1–O11	158.16(11)	C11–C17–N11	124.9(5)
S11–Fe1–O21	90.03(11)	C17–N11–Fe1	126.8(3)
S11–Fe1–N21	88.32(11)	Fe1–O21–C22	134.2(3)
S21–Fe1–O11	92.89(11)	O21–C22–C21	121.5(4)
S21–Fe1–O21	160.48(11)	C22–C21–C27	123.5(4)
S21–Fe1–N11	84.89(11)	C21–C27–N21	125.6(4)
S21–Fe1–N21	79.05(11)	C27–N21–Fe1	126.3(3)
O11–Fe1–O21	84.89(15)	C18–S11–Fe1	99.81(17)
O11–Fe1–N11	83.71(14)	N11–N12–C18	120.4(4)
O11–Fe1–N21	112.13(14)	N12–C18–S11	121.3(4)
O21–Fe1–N11	114.03(15)	C28–S21–Fe1	99.60(17)
O21–Fe1–N21	83.82(14)	N21–N22–C28	121.2(4)
N11–Fe1–N21	157.80(15)	N22–C28–S21	120.9(4)
Fe1–O11–C12	134.9(3)		

Table 3

Hydrogen-bond geometry (Å, °)

D	H	A	d(D-H)/Å	d(H-A)/Å	d(D-A)/Å	D-H-A/deg
N12	H12	O202	0.87(3)	1.92(4)	2.733(6)	155(5)
N13	H13	O203	0.88(3)	2.02(3)	2.890(6)	176(5)
N22	H22	O101[1]	0.87(3)	1.85(3)	2.695(6)	166(5)
N23	H23	O201[2]	0.87(3)	2.23(4)	2.887(6)	133(4)
O101	H10A	O202[1]	0.85	1.90	2.692(6)	155.2
O101	H10B	O11	0.85	2.28	2.809(6)	120.9

Symmetry codes:

[1]-1/2+x,+y,1-z; [2]-1+x,3/2-y,3/2-z

Scheme 1

Figure 1 ORTEP projection showing the molecular structure and the atom-numbering scheme for (I). Displacement ellipsoids are drawn at the 50% probability level.

Figure 2 ORTEP projection showing the hydrogen bonding interactions of (I). Displacement ellipsoids are drawn at the 50% probability level. Dashed lines indicate hydrogen bonds. [Symmetry codes: (i) x + 1, –y + 1/2, –z + 3/2; (ii) x – 1/2, y, –z + 1; (iii) x, –y + 1/2, –z + 3/2].

Figure 3 ORTEP projection showing the unit cell of (I). Displacement ellipsoids are drawn at the 50% probability level.

Figure 4 (a) $\chi_M T$ vs T for (I). The data were measured while heating at a rate of in a 2 K min^{-1} in an applied field $\mu_0 H$, of 0.1 T. (b) Temperature dependence of the corresponding molar magnetic susceptibility, χ_M, for (I). The solid red lines show fits to the data using Equation (1), with D = 0.439(1) cm^{-1} and g = 2.0. The blue line in Figure 4(b) shows a fit of $\chi_M^{-1}(T)$ above 100 K using a Curie-Weiss law.

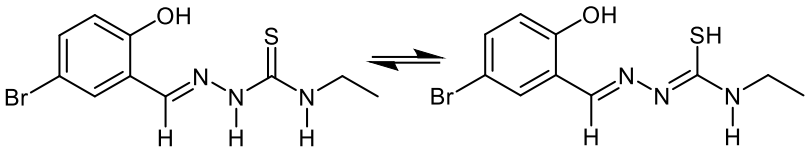

Scheme 1

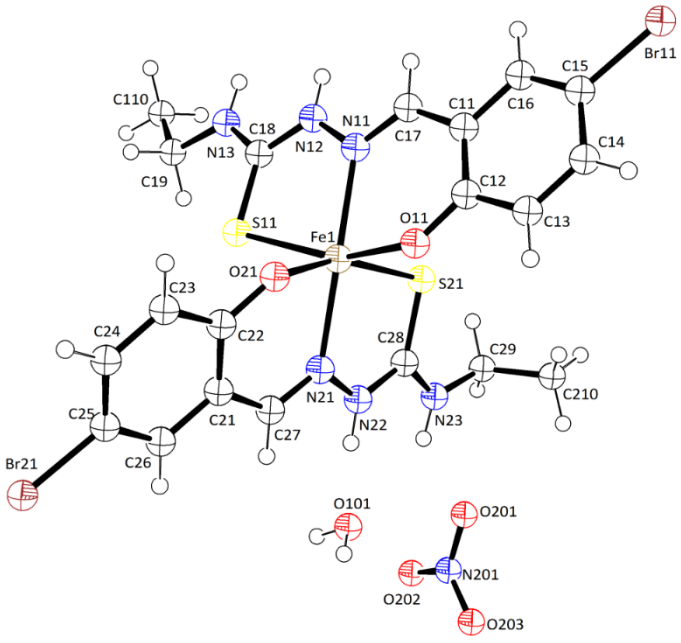

Figure 1 ORTEP projection showing the molecular structure and the atom-numbering scheme for (I). Displacement ellipsoids are drawn at the 50% probability level.

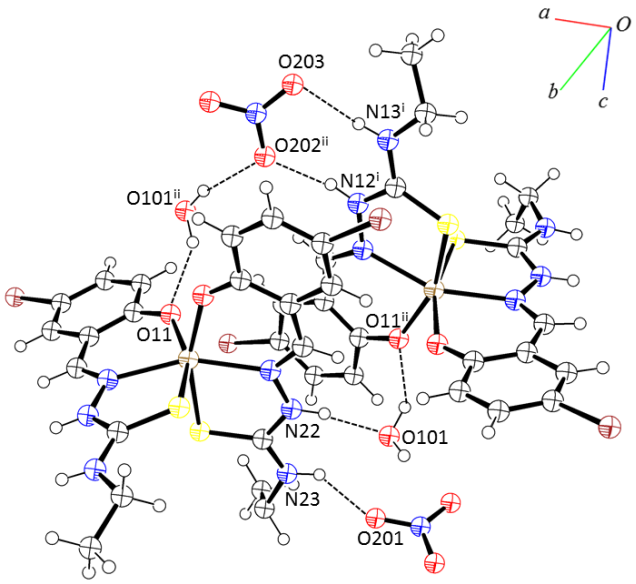

Figure 2 ORTEP projection showing the hydrogen bonding interactions of (I). Displacement ellipsoids are drawn at the 50% probability level. Dashed lines indicate hydrogen bonds. [Symmetry codes: (i) x + 1, –y + 1/2, –z + 3/2; (ii) x – 1/2, y, –z + 1; (iii) x, –y + 1/2, –z + 3/2].

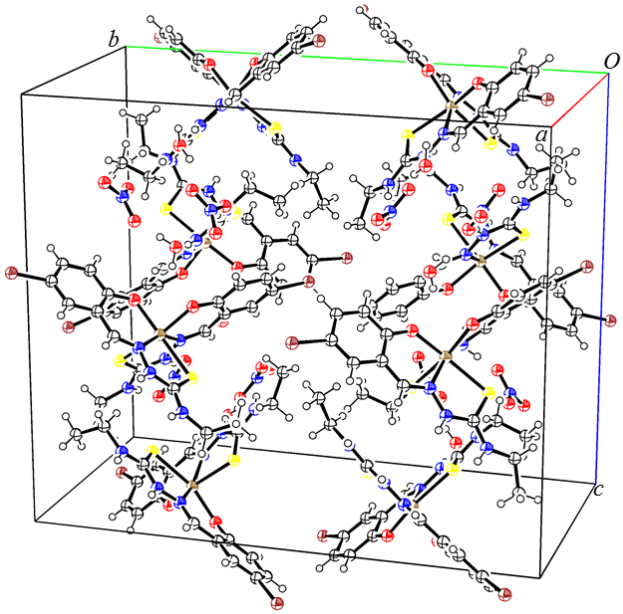

Figure 3 ORTEP projection showing the unit cell of (I). Displacement ellipsoids are drawn at the 50% probability level.

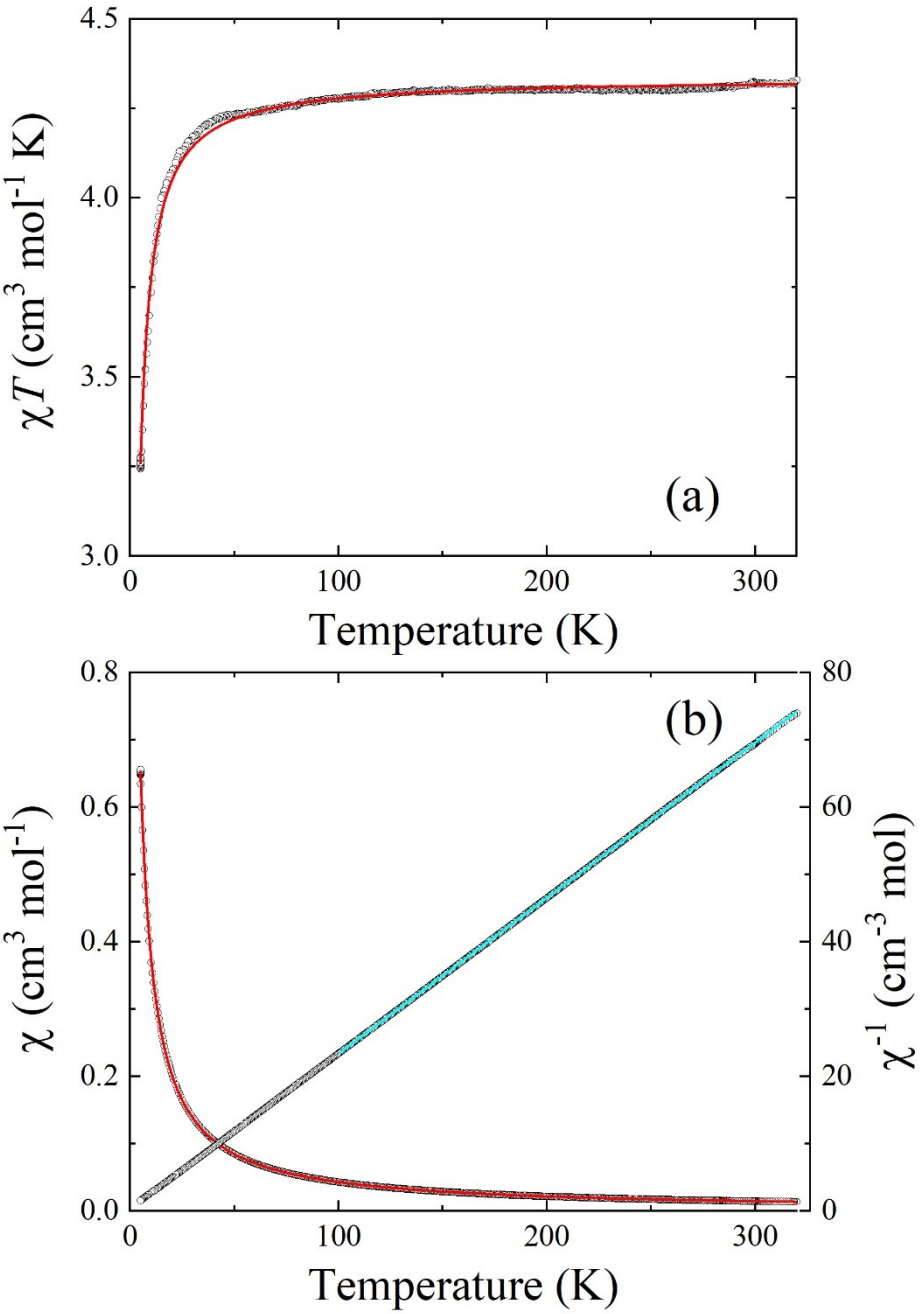

Figure 4 (a) $\chi_M T$ vs T for (I). The data were measured while heating at a rate of in a 2 K min^{-1} in an applied field $\mu_0 H$, of 0.1 T. (b) Temperature dependence of the corresponding molar magnetic susceptibility, χ_M, for (I). The solid red lines show fits to the data using Equation (1), with D = 0.439(1) cm^{-1} and g = 2.0. The blue line in Figure 4(b) shows a fit of $\chi_M^{-1}(T)$ above 100 K using a Curie-Weiss law.

Supporting information

S1. Computing details

Diffractometer: *Rigaku AFC12* goniometer equipped with an enhanced sensitivity (HG) *Saturn724+* detector mounted at the window of an *FR-E+ SuperBright* molybdenum rotating anode generator with HF *Varimax* optics. **Cell determination and data collection**: *CrystalClear-SM Expert 3.1 b27* (Rigaku, 2013). **Data reduction, cell refinement and absorption correction**: *CrysAlisPro 1.171.141.120a* (Rigaku OD, 2021). **Structure solution**: *SHELXT 2018/2* (Sheldrick (2015)). **Structure refinement**: *SHELXL 2018/3* (Sheldrick (2015)). **Graphics:** *OLEX2* (Dolomanov *et al.* (2009)), *ORTEP-3* for Windows (Farrugia, (2012)).

Table S1

C_{20} H_{24} Br_2 Fe N_7 O_6 S_2 [+ solvent]	Mo Kα radiation
M_r = 738.25	λ = 0.71075 Å
Orthorhombic	Cell parameters from 13504 reflections
Pnna	Θ = 2.135 - 27.485°
a = 12.3595(3) Å	μ = 3.559 mm^{-1}
b = 23.2686(6) Å	T = 100 K
c = 19.6406(6) Å	Dark green, lath
α = 90°	0.19 x 0.01 x 0.01 mm
β = 90°	
γ = 90°	
V = 5648.4(3) $Å^3$	
Z = 8	
D_x = 1.736 g cm^{-3}	
D_m not measured	

Data collection

Rigaku Saturn724+ diffractometer	R_{int} = 0.0875
Absorption correction:	Θ_{max} = 27.485°
T_{min} = 0.73967, T_{max} = 1.00000	h = -15 → 16
36848 measured reflections	k = -30 → 28
6477 independent reflections	l = -25 → 22
4297 observed reflections	

[F > 2σ(F)]

Refinement

Refinement on F^2	$w = 1/[\sigma^2(F_o^2) + (0.0514P)^2+12.8609P]$ Where $P = (F_o^2 + 2F_c^2)/3$
R1 = 0.0572	
wR2 = 0.1300	$\Delta\rho_{max}$ = 0.683 e Å^{-3}
S = 1.014	$\Delta\rho_{min}$ = ─0.779 e Å^{-3}
6477 reflections	Extinction correction: none
348 parameters	H atoms were refined with the riding model
6 restraints	